AN ASCA STUDY OF THE COMPOSITE SUPERNOVA REMNANT G18.95-1.1

NASA Grant NAG5-8394

Final Report

For the Period 15 March 1999 through 14 March 2000

Principal Investigator
Ilana Harrus

March 2000

Prepared for:

National Aeronautics and Space Administration
Goddard Space Flight Center
Greenbelt, MD 20771

Smithsonian Institution
Astrophysical Observatory
Cambridge, Massachusetts 02138

The Smithsonian Astrophysical Observatory
is a member of the
Harvard-Smithsonian Center for Astrophysics

The NASA Technical Officer for this grant is Donald K. West, 681.00, National Aeronautics and Space Administration, Goddard Space Flight Center, Greenbelt, MD 20771-0001.

This is the final report on the work done on Supernova Remnant (SNR) G18.95−1.1. The data were taken on April, 2, 1998 and delivered a couple of months later to the Principal Investigator (PI: Dr. Ilana Harrus). We received a CD-ROM containing the results of the standard processing pipeline and all the files needed for the analysis.

We have analyzed the data and presented a poster on this object at the 194th American Astronomical Society Meeting in Chicago (June 1999). A copy of the poster is appended to this report.

The poster presentation triggered several discussions and we are summarizing the analysis results and those discussions in a paper to be submitted soon to the Astrophysical Journal.
We have appended the draft of the paper to this report. It must be noted that the paper is still in its early stages. In particular more work is needed in the physical implications of the results of the spectral analysis and in the comparison with theoretical models to understand the curious morphology of the remnant.

The project should be completed within the next two months.

Explaining the morphology of centrally brightened Supernova Remnants (SNRs).

ASCA study of G18.95-1.1 & G272.2-3.2

Ilana M. Harrus[1], Patrick O. Slane[1] &
John P. Hughes[2]

[1] Harvard-Smithsonian Astrophysical Observatory, 60 Garden St. Cambridge, MA 02138, U.S.A.

[2] Rutgers University, 136 Frelinghuysen Rd. Piscataway, NJ 08854-8019, U.S.A.

imh@head-cfa.harvard.edu

THE RESULTS!

WHY ARE WE DOING THIS?

HOW WE ARE DOING THIS?

G18.95-1.1

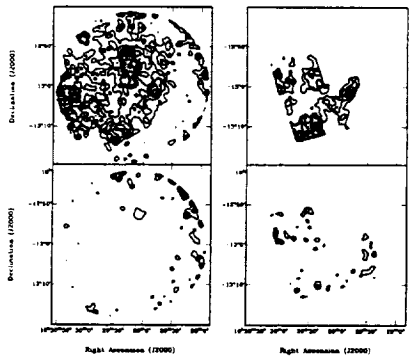

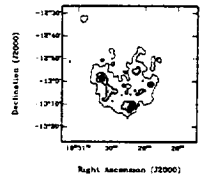

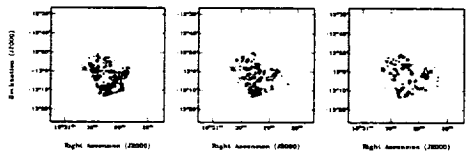

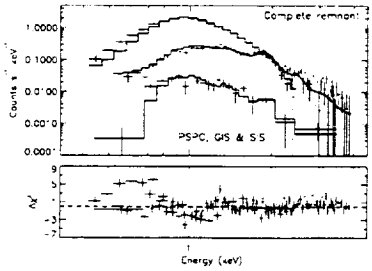

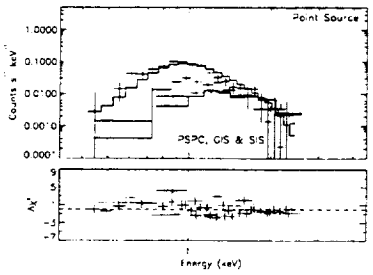

Summary for G18.95-1.1

General Picture

G272.2-3.2

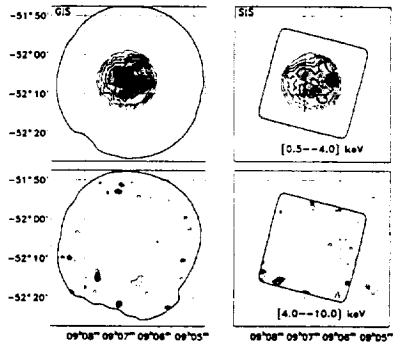

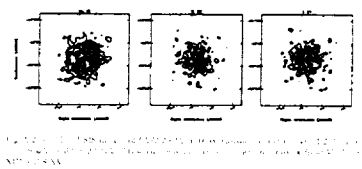

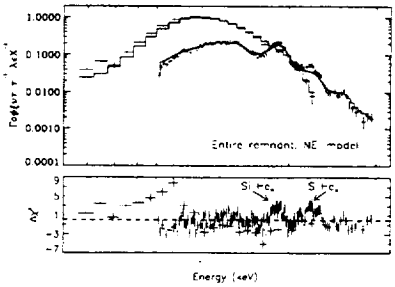

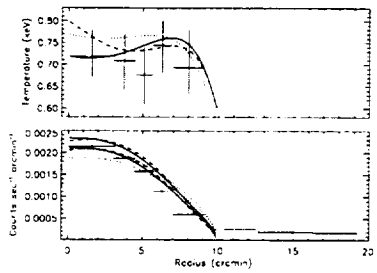

Summary for G272.2-3.2

General Picture

References

If only life was that simple...

FOR PUBLICATION IN THE ASTROPHYSICAL JOURNAL.
Preprint typeset using LaTeX style emulateapj

ASCA STUDY OF THE CENTRALLY-PEAKED THERMAL SUPERNOVA REMNANT: G18.95−1.1

ILANA HARRUS[1] AND PATRICK O. SLANE[2]

For publication in the Astrophysical Journal.

ABSTRACT

We present a combined analysis of data from the *Advanced Satellite for Cosmology and Astrophysics* (*ASCA*) of the supernova remnant (SNR) G18.95−1.1. We find that this remnant can be classified as a "thermal composite" remnant and is characterized by a thermal X-ray spectrum coupled with a centrally-bright morphology.

G18.95−1.1 was observed by the *ROSAT* PSPC and its spectrum could not be fitted by a single temperature collisional-plasma model. A point source also appears in the *ROSAT* PSPC image. We find no evidence of a high-energy component anywhere in the remnant. The total spectrum can be described by a thermal model at a temperature around 0.60 keV, associated with a column density of about 8×10^{22} atoms cm^{-2}. The *ASCA* spectrum extracted from the *ROSAT* point source is essentially similar to that of the remnant. We interpret it as a temperature variation in the remnant.

The centrally peaked aspect of the remnant is fitted using both a model of cloud evaporation and a thermal conduction model. At a 2 kpc distance, G18.95−1.1 is still young (around 6000 years old) but presents the puzzle of an under-luminous initial energy explosion. We discuss these results in the context of SNRs evolution.

Subject headings: ISM: individual (G18.95−1.1) — supernova remnants — X-rays: interstellar

1. INTRODUCTION

A detailed radio map of G18.95−1.1 with an angular resolution of 69″) was obtained by Fürst, Reich & Aschenbach (1997) using the Effelsberg 100-m telescope. The result of their observation is presented in Fig 1. It shows a distinct central bar, polarized surrounded by a shell of diffuse emission. Results from the analysis of the radio data confirm earlier results (Fürst et al. 1989) that about 80% of the radio emission is in the diffuse component with a total flux of about 20.4±0.2 Jy (measured at 10.55 GHz). This result is consistent with the existing radio data at 1.4GHz and 4.75 GHz. The spectral index extracted from these measurement is α = -0.14±0.03 for the diffuse component and α = -0.22±0.07 for the central bar, so essentially similar within the error bar. One part of the remnant (a prominent northern arc - see Fig 1) has a steeper spectral index of α = -0.36±0.04. The linear polarization across the remnant is about 6% at 10.55 GHz a little more than twice that at 4.75 GHz. The polarization intensity is highly concentrated: when the diffuse contribution is subtracted, the polarization in the central bar increases to about 40% in the central bar and in the arc.

This SNR was observed by the *ROSAT* PSPC for 12 ksec (Fürst et al. 1997). We have extracted the data from the public archive and produced a contour plot of the soft x-ray emission from the SNR (Fig 2). A point source is detected within the bounds of the SNR at at $18^h28^m48^s$, −13°00′55″ (J2000). The source has no optical or radio counterparts. With only 618 counts from the point source, no timing analysis was possible. We have extracted the spectrum for a circular region around this point source and we find that it can be fitted by a collisional-plasma model (Raymond-Smith model) with solar abundances with a column density of $0.70^{+0.55}_{-0.60}\times10^{22}$ atoms cm^{-2} and an associated temperature of 0.60±0.40 keV. In comparison, the spectrum extracted from the edge of the SNR leads to a column density of ($N_H = 1.05^{+0.20}_{-0.35}\times10^{22}$ atoms cm^{-2}) and a temperature of $0.35^{+0.30}_{-0.10}$ keV. A pure power-law fit of the spectrum from the point source is excluded because of the steep slope required ($\alpha \simeq 9.9$) in this case.

The complete spectrum from the remnant cannot be accurately fitted by a single temperature collisional-plasma model: in this case the χ^2_r is larger than 2.2 (the column density is $1.06\pm0.07\times10^{22}$ atoms cm^{-2} and the temperature is 0.37±0.06 keV). The spectrum is best fitted ($\chi^2_r \simeq 0.87$) with a 2-temperature collisional-plasma model. The column density found in this case ($0.44\pm0.30\times10^{22}$ atoms cm^{-2}) is in agreement with the limit imposed by HI data. The two temperatures associated are $0.26^{+0.60}_{-0.20}$ and $1.1^{+1.25}_{-0.30}$ keV. Despite the good χ^2 found in this case, the fit remains unsatisfactory as shown by the large errors bars associated with the two temperatures found in this case.

The results of the analysis by Fürst et al. (1997) lead to a very low age for the SNR associated with a small swept-up mass (around 5 $M_\odot$) and a relatively low initial explosion energy. For such low swept-up mass, it is difficult to assert the validity of the Taylor-Sedov set of solutions, both for the measured temperature and the age derived from it.

We have analyzed *ASCA* data on SNR G18.95−1.1 and described how the new data fit within the picture of the remnant. We present in §2 our data extraction methods and spatial, and spectral analyses. In §3 we discuss the implications of our analysis. The final section of the article is a summary of our principal conclusions.

2. DATA REDUCTION AND ANALYSIS

G18.95−1.1 was observed by *ASCA* on April, 2, 1998. We privileged a double exposure of the point source with the 2 CCD cameras on-board the satellite, over the complete coverage of the remnant using complementary 2CCD mode with the

[1]NASA/USRA Goddard Space Flight Center, Greenbelt, MD, 20771
[2]Harvard-Smithsonian Center for Astrophysics, 60 Garden Street, Cambridge, MA 02138

SIS (given that the remnant is about 33′in diameter). The GIS covers the source completely.

We used the standard processed data as provided by the *ASCA* Guest Observer Facility (see "Guide for *ASCA* data reduction" at
http://heasarc.gsfc.nasa.gov/docs/frames/asca_proc.html
for more information on the cuts applied to the data). The event processing configuration was chosen to get the best opportunity for a clean spectral analysis, so we kept the rise-time configuration to the default. This resulted in a GIS time resolution of 0.125 s (the SIS is not used for timing analysis).

2.1. *Spatial Analysis*

We have generated exposure-corrected, background-subtracted images of the GIS and SIS data in soft (below 4.0 keV) and hard (above 4.0 keV) energy bands for the ∼ 25 ks observation. For the GIS, we have used newly generated blank maps to generate the background. These maps are more complete that the standard "high latitude" ones used in similar studies. They have been corrected for spurious point sources and are screened using the standard event screening criteria (for more details on the generation of these files, see
http://heasarc.gsfc.nasa.gov/docs/asca/mkgisbgd/mkgisbgd.html)
There is no equivalent routine for the SIS and we used the standard "blank maps". Exposure maps (both for GIS and SIS) are generated using ascaeffmap and ascaexpo programs. Both programs are part of the standard *ASCA* FTOOLS package available at
http://heasarc.gsfc.nasa.gov/docs/software/ftools/asca.html.

Events from regions of the merged exposure map with less than 10% of the maximum exposure were ignored. Merged images of the source data, background, and exposure were smoothed with a Gaussian of standard deviation, $\sigma = 45''$. We subtracted smoothed background maps from the data maps and divided by the corresponding exposure map. Fig. 3 shows the results of this procedure for both the SIS and the GIS detectors. One first thing to notice is that the remnant is undetected above 4 keV. This first simple fact will be used in the following spectral analysis. It already indicates that the "plerion" hypothesis for the centrally brightened remnant is less than likely. The GIS low-energy image, covering all the remnant, shows two maxima of emission located respectively at $18^h29^m15.6^s$, -12°55′22.5″ and $18^h28^m49.9^s$, -13°01′7.44″ (2000). The first maximum is located at the edge and coincide with the edge of the remnant as defined in the *ROSAT* image. The second maximum is aligned with the point source detected in the archival *ROSAT* data. We examine in the next section the spectral signatures from the different parts of the remnant.

2.2. *Spectral Analysis*

As seen in the spatial analysis, the remnant is undetected over 4.0 keV. Consequently we have restricted the energy range of all of the fits below this energy. We extracted X-ray spectra from circular regions centered at $18^h29^m23.72^s$, -13°00′44.76″ (J2000) for the GIS, using a radius of 11′7.4″ in the GIS. The region was chosen to encompass most of the emission from the SNR, and covers almost the totality of the existing *ROSAT* pointing, making a direct comparison between the two spectral studies possible. We have extracted the background from the same field of view, using part of the GIS which were not contaminated by the remnant. Although it does mean that the background extracted has a different off-axis distribution than the source spectrum, this method has the advantage of eliminating the high-energy contamination from the Galactic plan. The SIS observation is a bit trickier to analyze because of the CCD-chip boundaries and because the detector does not covers the complete remnant (the pointing was optimized for the study of the point source).
We extracted a spectrum from around the point source only and analyze it with the *ROSAT*-PSPC spectrum extracted around this point. The background used in the SIS analysis is also extracted from a latitude background file but we use parts of the chips to verify that the contamination from high-energy galactic contributions is negligible. The measured count rates are around 0.465±0.006 cnt sec^{-1} for the complete remnant (as measured with the GIS) and **±0.002 cnt sec^{-1} for point source in the SIS.

In the first part of our analysis, we have modeled the thermal emission with a collisional equilibrium ionization (CEI) model (the so-called "mekal" model - Mewe, Gronenschild & van den Oord 1985; Mewe, Lemen & van den Oord 1986; Kaastra 1992) which is available in the version 10.00 of XSPEC, the X-ray spectral analysis package used throughout this analysis. In all the thermal models used, we have kept the elemental abundances at their nominal values as defined by Anders & Grevesse (1989).

Absorption along the line of sight was taken into account with an equivalent column density of hydrogen, N_H, using the cross-sections and abundances from Morrison & McCammon (1983).

We separated the spectral analysis in two parts. The first concerns the study of the complete remnant as covered by the GIS. We first fit the *ASCA*-GIS spectra alone. The gain offset is allowed to vary (we measure a gain shift of -2.7% and a range of variation between -2.4% and -4.35calibration data analysis done by the *ASCA*-GIS team (see http://heasarc.gsfc.nasa.gov/docs/frames/asca_proc.html for more informations on calibration issues). We have used a pure thermal (CEI "mekal" model) to describe the emission and obtained a relatively good fit with a χ^2 of 283 (and a reduced $\chi^2_r = 1.93$). We find a column density of $(9.5\pm0.05)\times10^{21}$ atoms cm^{-2} higher than the value derived value from the *ROSAT* analysis (Fürst et al. 1997). One should note though that the lowest energy considered in the fit is 0.7 keV and so this value is not well constrain. We will see later on how this changes in the simultaneous fit of *ASCA*-GIS and *ROSAT*-PSPC. The temperature is consistent with previous studies (we find $kT=0.64^{+0.09}_{-0.04}$ keV). The unabsorbed flux in the [0.5-4.0] keV range is 2.13×10^{-10} ergs cm^{-2} s^{-1}, three order of magnitude higher than that in the [4.0-10.0] keV band.

We then fit *ASCA*-GIS and *ROSAT*-PSPC spectra simultaneously (the gain offset in the GIS is fixed to the value derived from the single GIS fit alone). *ROSAT*-PSPC data allow a stronger constrain on the column density value. We find $**\times10^{21}$ atoms cm^{-2}

The second part of the spectral analysis deals with the point source detected in the *ROSAT*-PSPC observation. We have analyzed its spectra extracted from both *ASCA*-SIS detectors, and the *ROSAT*-PSPC. As for the GIS, normalizations for both SIS detectors are kept linked.

We have also examined the effects of non-equilibrium ion-

ization (NEI) on our previous results. Non equilibrium effects arise when the ions are not instantaneously ionized to their equilibrium configuration at the temperature of the shock front. Rather, the timescale for attaining full equilibrium ionization is comparable to the remnant dynamical timescale. To incorporate these effects into the model of SNR spectral emissivity, we use here the matrix inversion method developed by Hughes & Helfand (1985). The ionization state depends on the product of electron density and age and we define the ionization timescale as $\tau_i \equiv n_e t$. As in the CEI model, we have kept all elements to their nominal abundances (Anders & Grevesse 1989). From the results obtained in the previous analysis, we can estimate an upper limit for the expected value of the ionization timescale. We find an upper limit for $n_e t$ between *** and *** yrs cm^{-3}. As in the CEI analysis, a single model fit cannot account for the total spectra. In the case of a single NEI model, we find χ^2= ** for ** degrees of freedom larger than the best χ^2 of the complete analysis but much better than the one obtained in the equilibrium case alone.

We have searched for variation of elemental abundances (in particular for Magnesium, Silicon and Sulfur) and found none. In addition, the temperature, ionization timescale and column density are similar to the ones found previously. Fig. 4 shows the data and the best-fit model for both the SIS and the GIS. Quantitative results and and fluxes are tabulated in Table 1.

3. DISCUSSION

Using a distance compatible with a distance to G18.95−1.1 around 2 kpc (Fürst et al. 1997), the supernova remnant defines an X-ray emitting volume of $V \simeq ** \times 10^{59} f D_2^3\ \theta_4^3$ cm^{-3}, where f is the volume filling factor of the emitting gas within the SNR, D_2 is the distance to the remnant in units of 2 kpc, and θ_4 the angular radius in units of 4′. From this estimate, the combined result from the thermal component (see Table 1), and a ratio $n_e/n_{\rm H}$ of 1.08 (extracted from our NEI analysis), we deduce a hydrogen number density of $n_{\rm H} = (0.{**}^{+0.**}_{-0.**}) D_2^{-1/2} \theta_4^{-3/2} f^{-1/2}$ cm^{-3}. The mass of X-ray emitting plasma is $M_X = ** D_2^{5/2} f^{1/2} \theta_4^{3/2}\ M_\odot$, which for the distance range mentioned above and combined with the errors from the spectral analysis, translates to a mass M_X between ** and *** $M_\odot$. Considering that the distances used are already a lower bound of the possible distance to the remnant, we argue that this result is consistent with the remnant being in its Sedov-Taylor phase of evolution (Taylor 1950; Sedov 1959). In this case, an estimate on the age of the remnant can be made using the temperature obtained in our spectral analysis. This temperature, $\langle T \rangle$, is the emission-measure-weighted average electron temperature, which is proportional to the shock temperature $\langle T \rangle = 1.27\ T_S$ (assuming that electrons and ions have the same temperature). The Sedov age relationship is $t \approx *** \mathrm{yrs} (R/1\,\mathrm{pc}) (\langle T \rangle / 1\,\mathrm{keV})^{-1/2} \approx ({***}^{+**}_{-**})$ yr (the errors bars reflect both the 1σ errors on the measured temperature and the uncertainties on the distance). The preshock ISM number density is $n_0 = \rho_0 m_{\rm H} = (0.{**}^{+0.07}_{-0.05}) D_{10}^{-1/2} \theta_4^{-3/2} f^{-1/2}$ cm^{-3}, which leads to $n_0 = (0.{**}^{+0.14}_{-0.10}) D_{10}^{-1/2} \theta_4^{-3/2}$ cm^{-3} for a filling factor of 0.25 (as expected in the case of a pure Taylor-Sedov solution). With the preceding numerical values we estimate the supernova explosion energy from the Taylor-Sedov relations to be $E = (**^{+1.5}_{-0.8}) \times 10^{50} D_{10}^{5/2} \theta_4^{3/2} f^{-1/2}$ ergs which is within the range of typical values.

Assuming temperature equilibrium between electrons and ions, we can compute the pressure at the shock front $P_s \sim$ ** $n_e k T_S \sim (1.29^{+0.61}_{-0.33}) \times 10^{-9} D_{10}^{-1/2} f^{-1/2}$ dyne cm^{-2}. For a Taylor-Sedov temperature and density distribution, the central pressure is $P_0 \sim 0.31 P_s = ** \times 10^{-10}$ dyne cm^{-2} for a filling factor of 0.25.

4. SUMMARY

We have presented the results of *ASCA* X-ray spectral and spatial studies of the SNR G18.95−1.1, a middle-aged remnant (about 7000 year old) in its Taylor-Sedov phase of evolution.

REFERENCES

Allen, G. et al 1997, ApJ 487, L97
Fürst, E., Reich, W., & Aschenbach, B. 1997, A & A, 319, 655
Fürst, E., Hummel, E., Reich, W., Sofue, Y., Sieber, W., Reif, K., & Dettmar, R. J. 1989, A & A, 209, 361
Kaastra, J. S. 1992, An X-Ray Spectral Code for Optically Thin Plasmas. Internal SRON-Leiden Report, updated version 2.0
Morrison, R. & McCammon, D. 1983, ApJ, 270, 119
Raymond, J. C. & Smith, B. W. 1977, ApJS, 35, 419
Sedov, L. I. 1959, Similarity and dimensional methods in mechanics, (New York: Academic Press)
Seward, F. D. & Wang, Z. R. 1988, ApJ, 332, 199
Taylor, G. I. 1950, Proc Royal Soc London, 201, 159

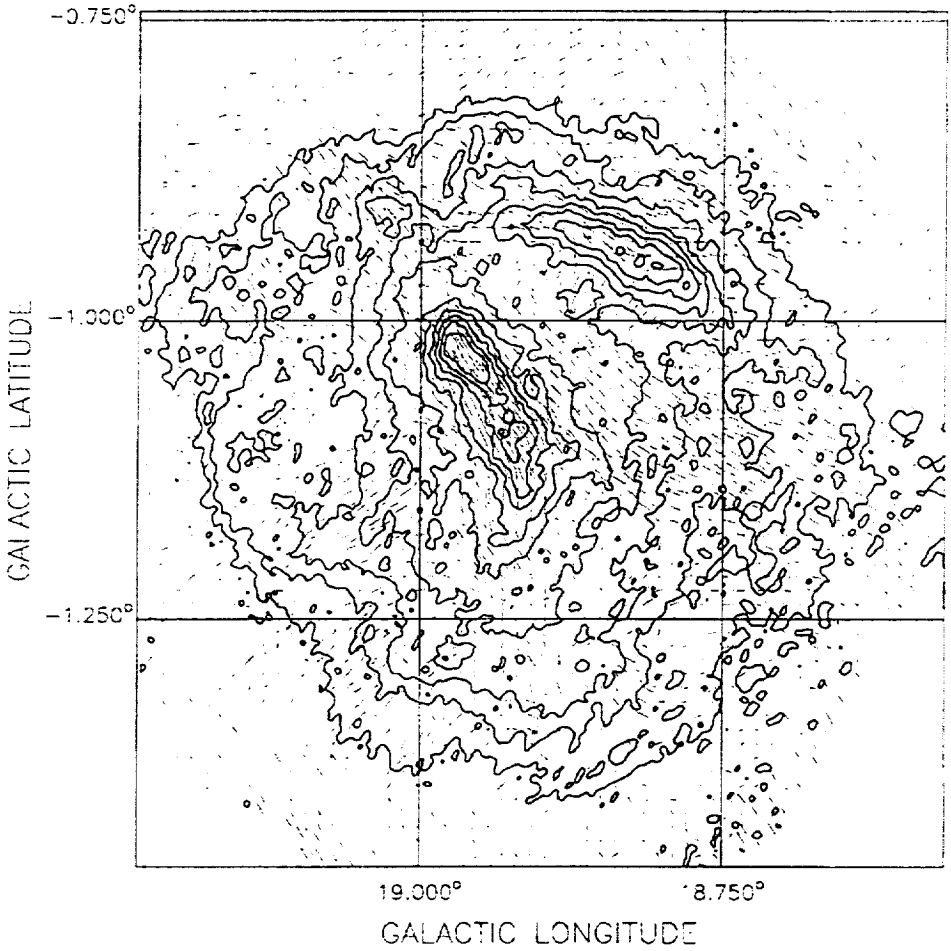

FIG. 1.— The radio contour map of G18.95−1.1 at 10.55 GHz (from Fürst et al. 1997). The magnetic field is overlaid as bars with the length proportional to the polarized intensity.

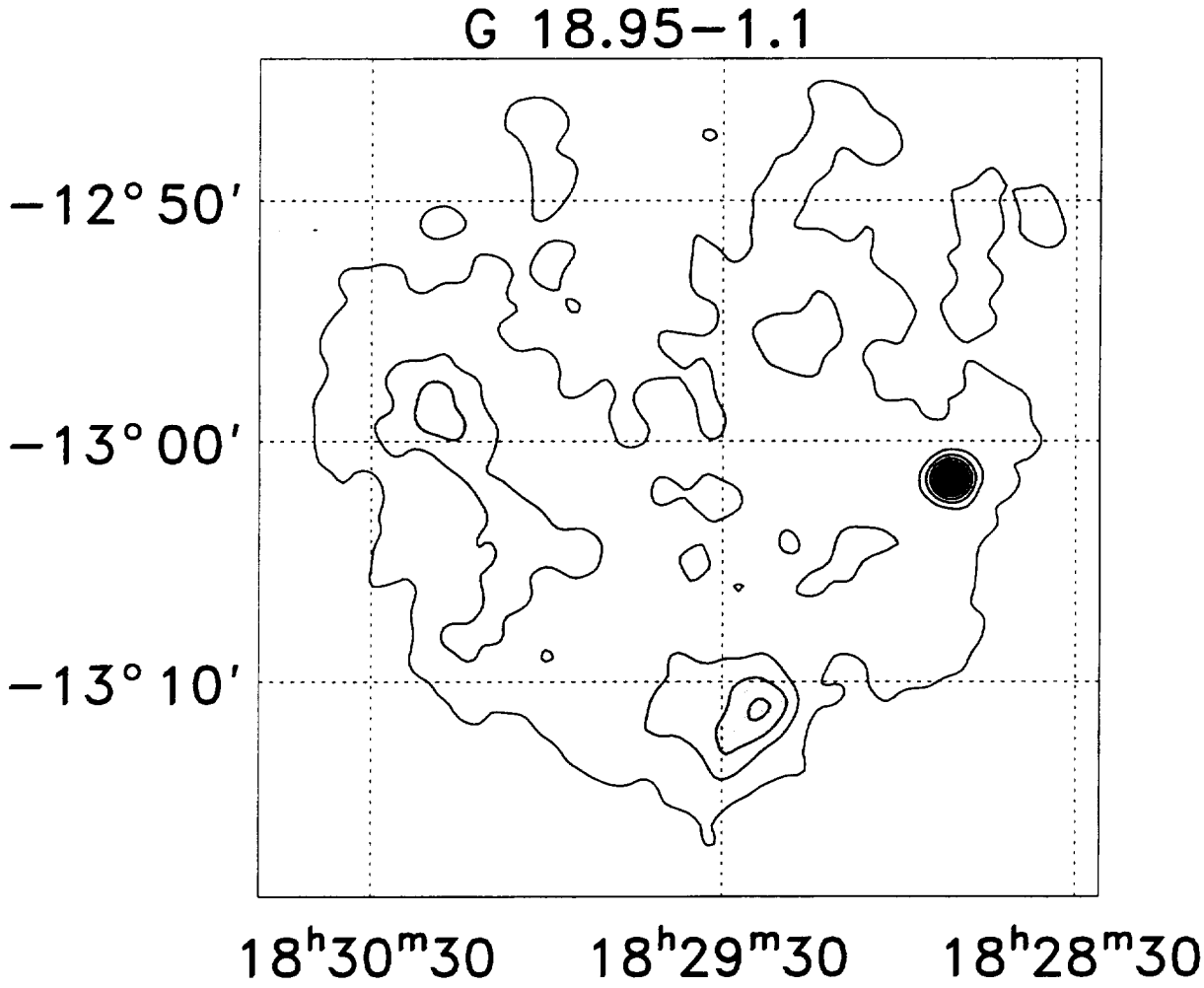

FIG. 2.— *ROSAT PSPC image of supernova remnant G18.95–1.1 - The image has been cleaned using Snowden procedure for studies of extended objects. The point source at the edge of the SNR is examined in the spectral analysis.*

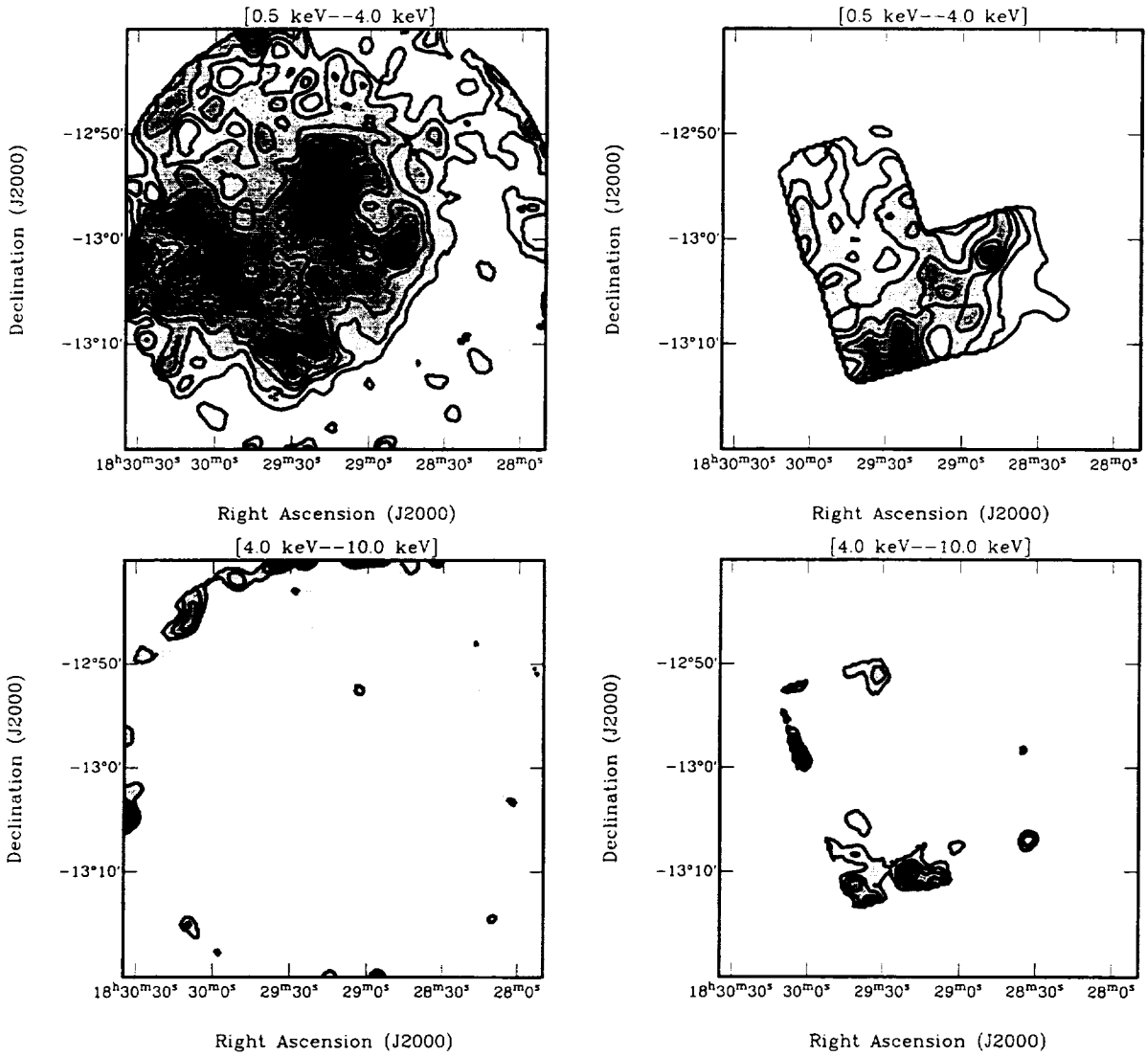

FIG. 3.— *ASCA* X-ray images of the SNR G18.95−1.1 at low and high energy (top: 0.5–4.0 keV; bottom: $\gtrsim$ 4.0 keV) for the GIS (left) and the SIS (right). Contour values are linearly spaced from 20% to 90% of the peak surface brightness in each map. Peak/background values are top: 4.2/0.7; bottom: 0.3/0.17 for the GIS and top: 7.5/1.6; bottom: 0.8/1.2 for the SIS, where all values are quoted in units of 10^{-3}counts s^{-1} $arcmin^{-2}$.

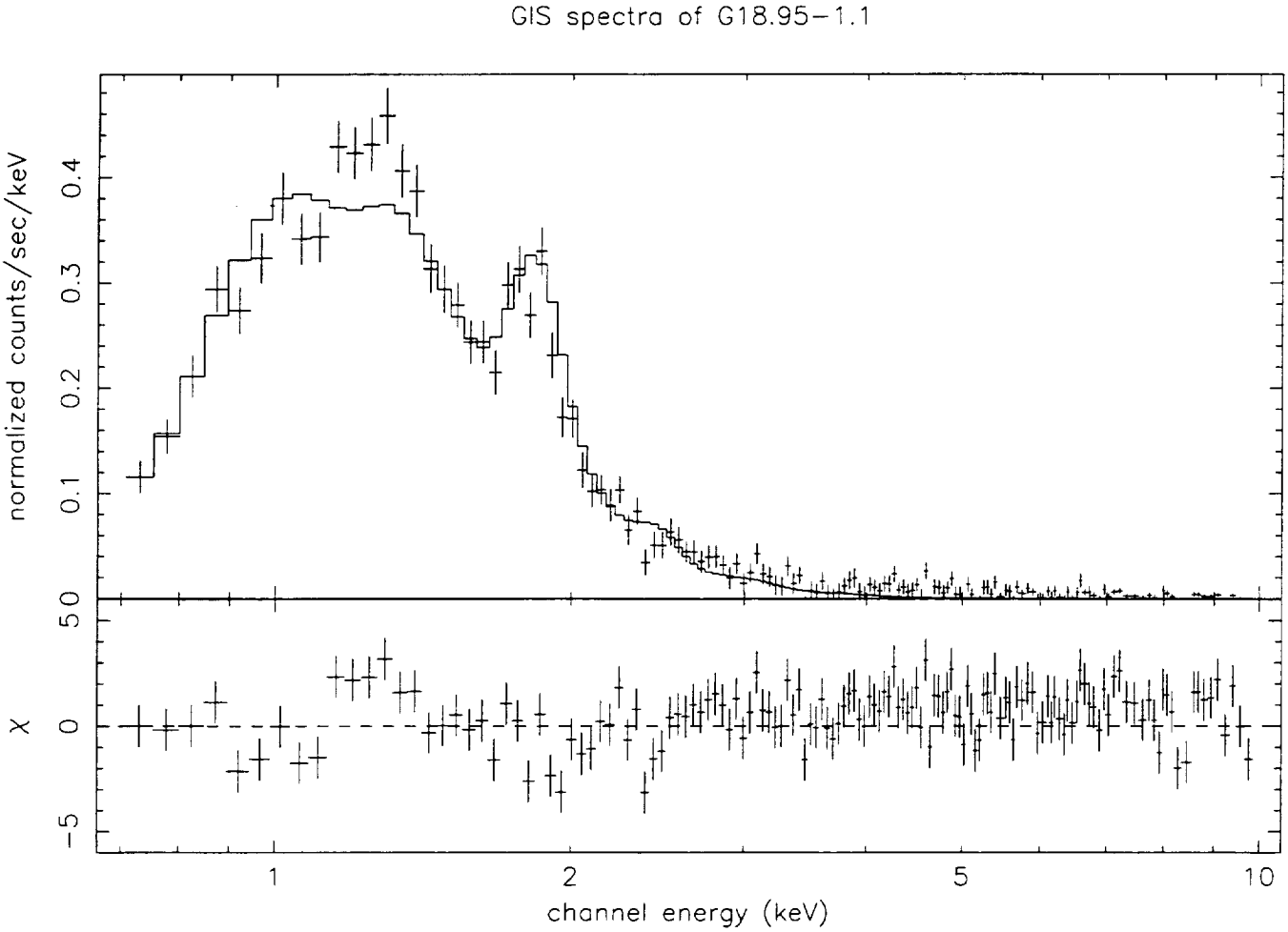

FIG. 4.— GIS spectra of G18.95−1.1 extracted from a 11.1′ radius circular region. The solid curve in the top panel shows the best-fit. The bottom panel shows the data/model residuals.